


Article

Polyketide Derivatives from the Endophytic Fungus *Phaeosphaeria* sp. LF5 Isolated from *Huperzia serrata* and Their Acetylcholinesterase Inhibitory Activities

Yiwen Xiao ^{1,2,†}, Weizhong Liang ^{2,†}, Zhibin Zhang ¹, Ya Wang ², Shanshan Zhang ², Jiantao Liu ², Jun Chang ², Changjiu Ji ³ and Du Zhu ^{1,2,*} 

¹ Key Laboratory of Protection and Utilization of Subtropic Plant Resources of Jiangxi Province, College of Life Sciences, Jiangxi Normal University, Nanchang 330022, China; xyw1152858687@163.com (Y.X.); zzbio@jxnu.edu.cn (Z.Z.)

² Key Laboratory of Bioprocess Engineering of Jiangxi Province, College of Life Sciences, Jiangxi Science and Technology Normal University, Nanchang 330013, China; lwz271508312@163.com (W.L.); jxwangya@126.com (Y.W.); zss18135437140@163.com (S.Z.); liujt@jxstnu.edu.cn (J.L.); changjun@jxstnu.edu.cn (J.C.)

³ College of Chemistry and Biological Engineering, Yichun University, Yichun 336000, China; jichjiu999@jycu.edu.cn

* Correspondence: zhudu@jxstnu.edu.cn; Tel.: +86-79-188121934

† These authors contributed equally to this work.

Abstract: The secondary metabolites of *Phaeosphaeria* sp. LF5, an endophytic fungus with acetylcholinesterase (AChE) inhibitory activity isolated from *Huperzia serrata*, were investigated. Their structures and absolute configurations were elucidated by means of extensive spectroscopic data, including one- and two-dimensional nuclear magnetic resonance (NMR), high-resolution electrospray ionization mass spectrometry (HR-ESI-MS) analyses, and calculations of electronic circular dichroism (ECD). A chemical study on the solid-cultured fungus LF5 resulted in 11 polyketide derivatives, which included three previously undescribed derivatives: aspilactonol I (**4**), 2-(1-hydroxyethyl)-6-methylisonicotinic acid (**7**), and 6,8-dihydroxy-3-(1'*R*, 2'*R*-dihydroxypropyl)-isocoumarin (**9**), and two new natural-source-derived aspilactonols (G, H) (**2**, **3**). Moreover, the absolute configuration of de-*O*-methyladiaporthin (**11**) was identified for the first time. Compounds **4** and **11** exhibited inhibitory activity against AChE with half maximal inhibitory concentration (IC₅₀) values of 6.26 and 21.18 μM, respectively. Aspilactonol I (**4**) is the first reported furanone AChE inhibitor (AChEI). The results indicated that *Phaeosphaeria* is a good source of polyketide derivatives. This study identified intriguing lead compounds for further research and development of new AChEIs.

Keywords: *Phaeosphaeria* sp.; secondary metabolite; polyketide; AChE inhibitor; biosynthetic pathways



Citation: Xiao, Y.; Liang, W.; Zhang, Z.; Wang, Y.; Zhang, S.; Liu, J.; Chang, J.; Ji, C.; Zhu, D. Polyketide Derivatives from the Endophytic Fungus *Phaeosphaeria* sp. LF5 Isolated from *Huperzia serrata* and Their Acetylcholinesterase Inhibitory Activities. *J. Fungi* **2022**, *8*, 232. <https://doi.org/10.3390/jof8030232>

Academic Editors: Tao Feng and Frank Surup

Received: 3 February 2022

Accepted: 24 February 2022

Published: 26 February 2022

Publisher's Note: MDPI stays neutral with regard to jurisdictional claims in published maps and institutional affiliations.



Copyright: © 2022 by the authors. Licensee MDPI, Basel, Switzerland. This article is an open access article distributed under the terms and conditions of the Creative Commons Attribution (CC BY) license (<https://creativecommons.org/licenses/by/4.0/>).

1. Introduction

Natural products are important sources of active compounds and play important roles in modern drug research and development. Fungi are considered an important group of microorganisms in the production of antitumor, immunosuppressant, antibiotic, antifungal, antiparasitic, anti-inflammatory, enzyme-inhibiting, and other active secondary metabolites [1,2]. Endophytic fungi reside in the internal tissues of living plants without causing apparent disease. Due to their unique ecological niche, endophytic fungi have become important sources of natural products to be screened for with unique chemical structures and biological activity [3,4]. Therefore, the natural product screening of endophytic fungi is currently a hot research topic [5–9]. In this sense, it is worth undertaking a constant search for novel compounds from endophytic fungal sources and paying attention to discovering potential drug candidates.

Huperzia serrata is a member of the *Lycophyllaceae* family called shezucuo in China [10]. Huperzine A (HupA) was first isolated from *H. serrata* in the 1980s and was approved in the 1990s in China as an acetylcholinesterase inhibitor (AChEI) to treat Alzheimer's disease (AD). These promising studies showed that endophytic fungi of *H. serrata* can synthesize HupA and similar compounds in host plants and also contains many novel compounds [10]. Thus far, many studies have been conducted on the diversity of endophytic fungi of *H. serrata*, but there are few studies on the isolation and screening of AChEIs in these endophytic fungi, and therefore further studies are needed. In our previous study, a total of 22 endophytic fungal strains showed strong AChE inhibitory activity ($\geq 50\%$) [11]. As part of our ongoing research, we are currently characterizing the bioactive secondary metabolites of these endophytic fungi.

Phaeosphaeria sp. LF5 is an endophytic fungus isolated from the leaves of *H. serrata* [12]. Members of *Phaeosphaeria* have afforded a variety of natural products, such as polyketides, peptides, and terpenes [13,14]. Herein, *Phaeosphaeria* sp. LF5 was selected for screening for new AChEI natural products. We re-fermented the strain in solid substrate fermentation medium and then isolated 11 polyketide derivatives, which included three new compounds, aspilactonol I (4), 2-(1-hydroxyethyl)-6-methylisonicotinic acid (7), and 6,8-dihydroxy-3-(1'*R*, 2'*R*-dihydroxypropyl)-isocoumarin (9), and two new natural source-derived aspilactonols (G, H) (2, 3). We also identified the absolute configuration of de-*O*-methyladiaporthin (11) for the first time (Figure 1). In addition, we detected their AChE inhibitory activity. Herein, the isolation, structural elucidation, and bioactivities of these isolated compounds are described.

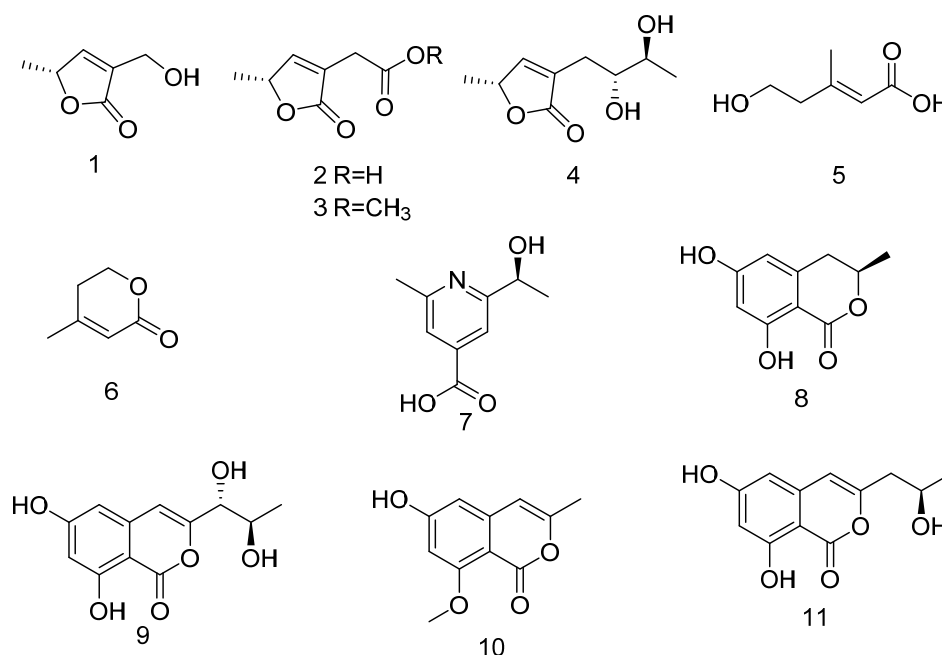


Figure 1. Chemical structure of compounds 1–11.

Generally, furanone derivatives are polyketide metabolites found in *Aspergillus* [15,16]. They are classified into three structural types: linear (aspinonene), δ -lactones (aspinrone), and γ -lactones (isoaspinonene and aspilactonols) [17]. To date, it has been a challenging task to assign the absolute configurations of furanone derivatives due to the flexibility of their aliphatic sidechain in the partial polyketide unit [18,19]. Isocoumarins comprise a six-membered oxygen heterocycle (α -pyranone) with one benzene ring. Isocoumarins represent a group of natural compounds rich in lactones, which are mainly derived from the fungal polyketone pathway. These compounds have exhibited a wide range of biological functions, including antifungal, anti-inflammatory, insecticidal, and hepatoprotective activities [20]. However, the determination of their absolute configuration becomes quite challenging

due to the high degree of free rotation of the steric centers on the chain, with the side chains connected to the nuclei of isocoumarin derivatives [21]. In the present study, the structures and absolute configurations of polyketide derivatives isolated from *Phaeosphaeria* sp. LF5 were elucidated by means of extensive spectroscopic data, including one- and two-dimensional nuclear magnetic resonance (NMR) spectrometry, high-resolution electrospray ionization mass spectrometry (HR-ESI-MS) analyses, and calculations of electronic circular dichroism (ECD).

2. Materials and Methods

2.1. General Experimental Procedures

Optical rotation values were determined on a JASCO P-1010 polarimeter (Jasco, Tokyo, Japan). UV spectra were recorded on a PerkinElmer Lambda 365 UV-Vis spectrophotometer (PerkinElmer, Hopkinton, MA, USA). High-resolution electrospray ionization mass spectrometry (HR-ESI-MS) data were measured on a Waters ACQUITY UPLC H-Class Q-TOF LC-MS spectrometer (Waters, Milford, MA, USA). High-performance liquid chromatography (HPLC) analysis was carried out on an ACQUITY UPLC H-Class System (quaternary solvent manager, sample manager, PDA detector, and ELS detector) using a YMC ODS (4.6 × 250 mm, 5 μm, 1 mL/min) column. MPLC was performed on a Puriflash450 (Interchim, Los Angeles, CA, USA) with a Flash C18 cartridge (50 μm, 40 g, YMC, Kyoto, Japan). Semipreparative HPLC was performed on a Waters 2535 Quaternary gradient module with a FlexInject, 2489 UV-VIS detector and Fraction Collector III (Waters, Milford, MA, USA). The NMR spectra were recorded on a Bruker Avance 400 MHz spectrometer using tetramethylsilane as the internal standard (Bruker, Ettlingen, Germany). Thin-layer chromatography (TLC) analyses were performed on glass precoated with silica gel GF254 glass plates. All reagents for the analysis were purchased from Xilong Scientific Co., Ltd. (Guangdong, China).

2.2. Fungal Material

The endophytic fungus *Phaeosphaeria* sp. LF5 was isolated from the leaves of *H. serrata* at the Chinese Academy of Sciences' Lushan Botanical Garden in Jiangxi Province, China [12]. This strain was deposited in the culture collection of the Key Laboratory of Protection and Utilization of Subtropical Plant Resources of Jiangxi Province, Jiangxi Normal University.

2.3. Fermentation and Extraction

The endophytic fungus LF5 was cultivated in 100 Erlenmeyer flasks (1000 mL); each flask contained 80 g of rice and 120 g of H₂O to create solid rice medium. The flasks were then static incubated at 28 °C for 40 days.

After the mycelia entered the static growth state, the rice solid fermentation was taken out of the Erlenmeyer flask, dried at 45 °C to remove the water, crushed before adding 80% ethanol, and ultrasonically agitated for 1 h. The static precipitation was filtered, and the above steps were repeated four times to obtain an ethanol extract. The filtrate was removed with a rotary evaporator (35 °C, 160 rpm). The ethanol crude extract was placed in 2000 mL of water and transferred to a separatory funnel. In turn, petroleum ether (PE), ethyl acetate (EA), and water-saturated butanol were used for extraction four times and were concentrated in vacuo to yield the combined crude extracts, PE extract (16.2 g), EA extract (76 g), n-butanol extract (105 g), and water extract (450 g).

2.4. Isolation and Purification

The EA extract (76.0 g) was dried and subjected to column chromatography on 200–300 mesh silica gel with different solvents of increasing polarity from PE to EA to MeOH to obtain eight fractions (Frs. 1–8) on the basis of TLC analysis.

Fraction 6 was purified by Sephadex LH-20 (GE Healthcare, Pittsburgh, PA, USA) (MeOH) to obtain three subfractions: Fr. 6.1–Fr. 6.3. Fraction 6.1 was further purified by semipreparative HPLC (CH₃OH/H₂O, 30:70, *v/v*) to yield **1** (12 mg, *t*_R = 4.0 min),

2 (9.5 mg, $t_R = 2.9$ min), and **3** (7 mg, $t_R = 7.0$ min). Fraction 8 was loaded onto a Sephadex LH-20 column and eluted with EA/CH₃OH (8:2) to yield two subfractions: Fr. 8.1 and Fr. 8.2. Subfraction Fr. 8.2 was separated by semi-preparative RP-HPLC (CH₃OH/H₂O, 10:90) to generate **4** (6.8 mg, $t_R = 11.0$ min) and **5** (4.0 mg, $t_R = 8.0$ min). Fraction 3 was separated by Sephadex LH-20 using CH₃OH as the eluting solvent and was then further purified via semipreparative HPLC CH₃OH/H₂O (30:70, *v/v*) to obtain compound **6** (2.9 mg, $t_R = 6.0$ min). Fraction 7 was further purified using Sephadex LH-20 (EA/CH₃OH, 90:10, *v/v*) to yield two subfractions: Frs. 7.1 and 7.2. Subfraction Fr. 7.1 was separated by semipreparative reversed-phase HPLC (RP-HPLC) (CH₃OH-H₂O, 5:95) to produce **7** (4.5 mg, $t_R = 4.5$ min). Fraction 2 (PE/EA 7:3) was separated into three subfractions (Fr. 2.1–2.3) with Sephadex LH-20 using MeOH as a mobile phase. Subfraction Fr. 2.1 was further purified via semipreparative HPLC using CH₃OH:H₂O (30:70) as a mobile phase at a flow rate of 5 mL/min to yield **8** (10 mg, $t_R = 36.0$ min). Subfraction Fr. 6.3 was separated by preparative HPLC (CH₃OH/H₂O, 30:70, *v/v*) to yield compounds **9** (8 mg, $t_R = 17$ min), **10** (5 mg, $t_R = 30.0$ min), and **11** (4 mg, $t_R = 45.0$ min).

2.5. Acetylcholinesterase Inhibitory Activity In Vitro Assay

The determination of the in vitro AChE inhibitory activity of the endophytic fungal extracts and compounds **1–11** was performed according to the spectrophotometry method developed by Ellman et al. [22] and modified by Ortiz et al. [23]. Rivastigmine and HupA, two known AChEIs, were used as positive controls. The assay was carried out in a 96-well microtiter plate reader. In brief, a preincubation solution of 250 μ L of phosphate buffer (200 mM, pH 7.7) that contained 15 μ L of purified compounds/HupA, 80 μ L of DTNB (3.96 mg of DTNB and 1.5 mg of sodium bicarbonate dissolved in 10 mL of phosphate buffer, pH 7.7), and 10 μ L of AChE was prepared. The mixture was incubated for 5 min at 25 °C. After preincubation, 15 μ L of the substrate AChI (10.85 mg in 5 mL of phosphate buffer) was added and incubated again for 5 min. The color developed was measured in a microwell plate reader at 412 nm (Molecular Devices, SpectraMax M2, San Jose, CA, USA). Percent inhibition was calculated through the following formula: (control absorbance–sample absorbance)/control absorbance \times 100. The IC₅₀ values were the means \pm SD of three determinations.

2.6. ECD Calculations

In general, conformational analyses were performed by random searching in Sybyl-X 2.0 using the MMFF94S force field with an energy cut-off of 5 kcal/mol (Sybyl Software, version X 2.0, 2013) [24]. The results showed the five lowest-energy conformers for compounds **4**, **7**, **9**, and **11**. Subsequently, geometric optimizations and frequency analyses were implemented at the B3LYP-D3(BJ)/6-31G* level in PCM MeOH using ORCA4.2.1 [25,26]. All conformers used for property calculations in this study were characterized as stable points on a potential energy surface with no imaginary frequencies. The excitation energies, oscillator strengths, and rotational strengths (velocity) of the first 60 excited states were calculated by the time-dependent density-functional theory (TD-DFT) at the PBE0/def2-TZVP level in MeOH. The ECD spectra were simulated by the overlapping Gaussian function (half the bandwidth at 1/e peak height, sigma = 0.30 for all) [27]. The Gibbs free energies for the conformers were determined by using thermal correction at the B3LYP-D3(BJ)/6-31G** level, and electronic energies were evaluated at the wB97M-V/def2-TZVP level in PCM MeOH using ORCA4.2.1 [25,26]. To obtain the final spectra, we used the Boltzmann distribution theory and the conformers' relative Gibbs free energy (ΔG) to average the simulated spectra. The absolute configuration of the only chiral center was determined by comparing the experimental spectra to the calculated molecular models.

3. Results and Discussion

Structure Elucidation

Compound **4**, a white powder soluble in methanol (MeOH), exhibited a pseudo-molecular ion peak at m/z 187.0965 $[M + H]^+$ (calculated for $C_9H_{15}O_4^+$: 187.0926) in the HR-ESI-MS spectrum, indicating a molecular formula of $C_9H_{14}O_4$, and two degrees of unsaturation. The 1H NMR data indicated two methyls at δ_H 1.20 (3H, d, $J = 6.1$ Hz, H-10) and 1.39 (3H, d, $J = 6.8$ Hz, H-6); one olefinic methane at δ_H 7.36 (1H, br s, H-4); and three oxymethines at δ_H 3.58 (1H, m, H-9), 3.60 (1H, m, H-8), and 5.09 (1H, br q, $J = 6.8$ Hz, H-5). The ^{13}C -NMR spectra revealed one ester carbonyl (δ_C 176.5), one olefinic methine (δ_C 154.2), one nonprotonated sp^2 carbon (δ_C 131.7), three oxygenated methines (δ_C 71.6, 74.8, and 79.8), one methylene (δ_C 29.6), and two methyls (δ_C 18.9 and 19.1).

The HMBC spectrum showed correlations between H-10 (δ_H 1.20)/C-8 (δ_C 74.8) and H-10 (δ_H 1.20)/C-9 (δ_C 71.6), as well as H-9 (δ_H 3.58)/C-7 (δ_C 29.6), H-9 (δ_H 3.58)/C-8, and H-9 (δ_H 3.58)/C-10. C-8 was correlated with C-3, C-7, and C-9 (Figure 2). When combined with the peak shape analysis of H-10 (δ_H 1.20, d, $J = 6.1$), C-9 was found to be connected to C-10, and C-8 was connected to C-9. Since C-8 and C-9 are methylene carbons and there is no nitrogen in the molecular formula, when combined with the chemical shift value, C-8 and C-9 were found to be connected to hydroxyl groups. H-7 is related to C-8, C-9, C-3, and C-4, and H-7 is methylene, but there were two groups of different H signals. Therefore, it can be inferred that one side of C-7 was connected to C-8. C-3 had the same characteristic signals as H-4, H-7, and H-8. The carbon shift signals of C-3 and C-4 were δ_C 131.7 and δ_C 154.2, respectively. HSQC indicated that C-4 was connected by protons, and it can be concluded that C-3 and C-4 were connected by a double bond and that C-4 was a quaternary carbon with two substitutions, one of which was connected with C-7. According to the HMBC cross-peak correlation of H-4/C-2 (δ_C 176.5), H-7/C-2, and C-3, we were able to infer that the side-chain fragment was attached to α,β -unsaturated- γ -lactone. HSQC indicated that C-2 was not connected to a proton. When combined with the molecular formula, C-4 was found to be a carbonyl group, H-4 was related to C-5, H-5 was related to C-6, and H-4 was related to HMBC. It was concluded that C-5 was connected to C-4, C-6 was connected to C-5, and the chemical shift value of C-5 was δ_C 79.8. When combined with the molecular formula, C-5 was also found to be connected to oxygen. Since the unsaturation degree of the compound was 2, the double bond between C-4 and C-3 occupied an unsaturation. An unsaturation remained, and there was no other double-bond carbon signal in the compound: hence, it is inferred that there was a cyclization system in which the chemical shift of C-2 was lower-field than that of the conventional carbonyl group. It was inferred that the other side of C-2 was connected to the oxygen and that C-5 and C-2 passed through the oxygen to form a lactone ring. The 1H (CD_3OD , 400 MHz) and ^{13}C -NMR (CD_3OD , 100 MHz) data are listed in Table 1.

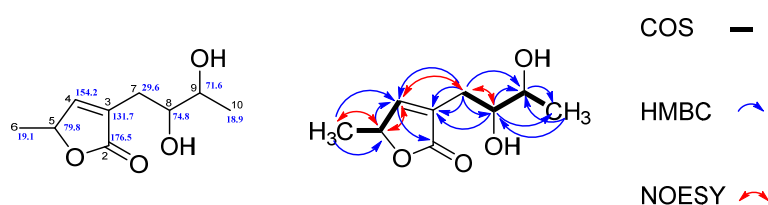


Figure 2. Signal assignments of compound **4** via ^{13}C and 2D NMR.

The ^{13}C chemical shift calculation was carried out at the B3LYP-D3(BJ)/6-31G** level to obtain the accurate relative configuration of **4**. In addition, the absolute configurations of **4** (5*R*, 8*R*, and 9*S*) were established by comparing electronic circular dichroism (ECD) calculations at the PBE0/def2-TZVP level with the experimental one (Figure 3). In addition, high correlation coefficients (R^2) between experimental and calculated chemical shifts were shown, with 0.9985 for **4** (Figure 4), indicating that the δ_C of **4** matched the calculated δ_C very well, which confirmed the framework of **4**. The structure of compound **4** was determined

to be (*R*)-5-((*8R*, *9S*)-8, 9-dihydroxybutyl)-5-methylfuran-2(5H)-one, so compound **4** was named aspilactonol I, as shown in Figure 1 (See Supplementary material).

Table 1. The ^1H , ^{13}C , HMBC, and HSQC NMR data for compound **4** in CD_3OD .

No.	^1H NMR	^{13}C NMR	HMBC	HSQC
2	—	176.5 (s)	H-4, H-7	—
3	—	131.7 (s)	H-4, H-7, H-8	—
4	7.36 (1H, br s)	154.2 (d)	H-5, H-6, H-7	7.36
5	5.09 (1H, br q, 6.8)	79.8 (d)	H-4, H-6	5.09
6	1.39 (3H, d, 6.8)	19.1 (q)	H-5	1.39
7	2.30 (1H, br dd, 15.2, 9.1); 2.59 (1H, br d, 15.2)	29.6 (t)	H-8, H-9	2.30, 2.59
8	3.60 (1H, m)	74.8 (d)	H-7, H-9, H-10	3.60
9	3.58 (1H, m)	71.6 (d)	H-8, H-10	3.58
10	1.20 (3H, d, 6.1)	18.9 (q)	H-8, H-9	1.20

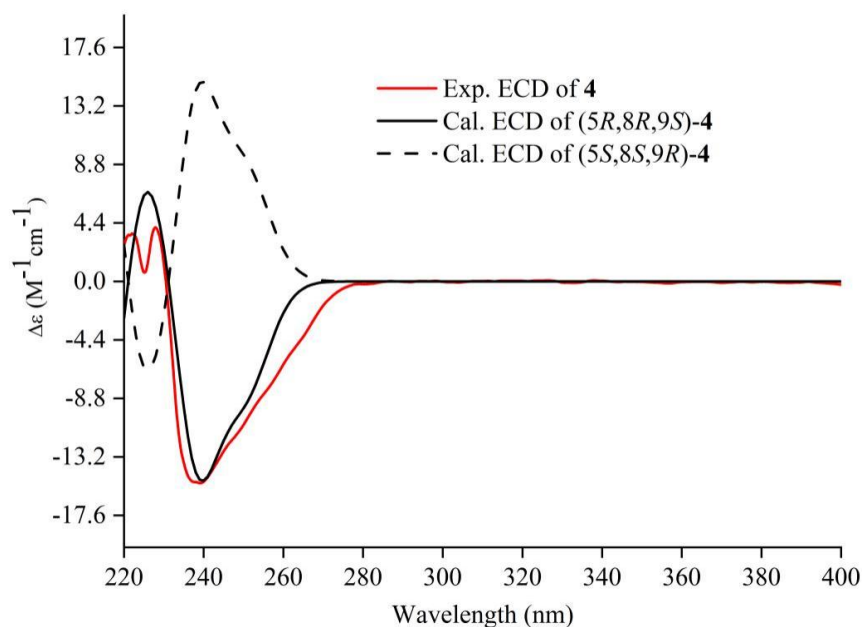


Figure 3. Experimental ECD spectra (200–400 nm) of **4** in MeOH and the calculated ECD spectra of the model molecules of **4** at the PBE0/def2-TZVP level.

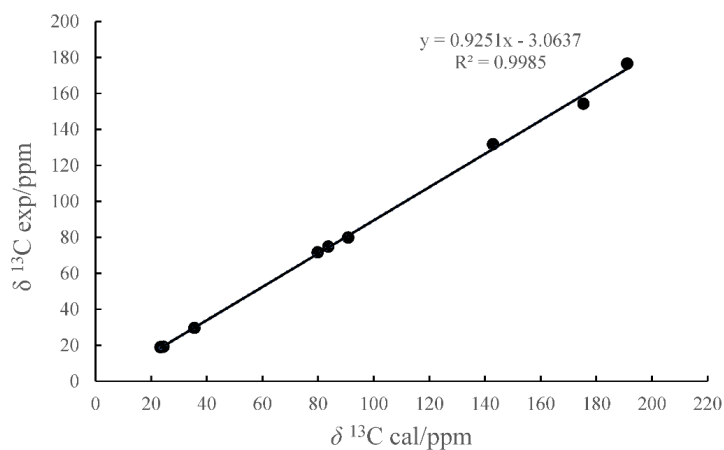


Figure 4. Calculated ^{13}C chemical shifts against the experimental data of **4**.

Compound 7, a white powder soluble in MeOH, has the molecular formula of $C_9H_{11}NO_3$ with four degrees of unsaturation from the protonated molecular ion at m/z 182.0810 $[M + H]^+$ (calculated for $C_9H_{12}NO_3^+$, 182.0812), as evidenced by HR-ESI-MS; the combination of ^{13}C -NMR and 1H -NMR spectra showed that the compound contained six low-field carbon signals, including four substituted low-field carbons, two unsubstituted aromatic carbons, one submethyl carbon, and two methyl carbons, including one methyl carbon directly connected to the aromatic ring. The compound is an alkaloid, as verified by the bismuth potassium iodide reaction. It is inferred that the compound contained a nitrogen-containing heterocyclic ring. According to the HMBC signal (Table 2), H-5 (δ_H 7.67) was correlated with C-6, C-3, and C-9, and H-3 was strongly correlated with C-2, C-5, and C-9. Furthermore, the HMBC-related signal intensity was weakly correlated. Combined with hydrogen spectrum signal splitting, C-3 and C-5 were interpositionally substituted, and H-3 and H-5 were weakly correlated with the C-9 signal intensity. H-5 was correlated with C-6 and C-10, and H-10 was strongly correlated with C-6, indicating that C-10 was linked to C-6, and the chemical shift of C-6 was lower than that of conventional aromatic carbonization. It is inferred that C-6 was linked to heteroatom N, resulting in a low chemical shift field, and H-3 and C-2 (δ_C 166.9) were detected. The correlation signal of H-7 with C-3 and C-8 and the correlation hydrogen spectrum signal of H-8 split (d) indicated that C-2 was connected with a hydroxyethyl, and the abnormal chemical shift of C-2 indicates that it was connected to N. After assignment of the related signals, it was found that C-4 (δ_C 142.2) did not generate any related signals, and there were two oxygens in the molecular formula of the compound that had not been attributed. Thus, it was inferred that the compound contained carboxylic acid groups. Since the unsaturation degree of the compound was 4 and it was a nitrogen-containing alkaloid, the carboxylic acid groups should be connected with the pyridine ring (Figure 5). The position of C-9 was determined according to the signal correlation between H-3, H-5, and C-9, and the paraposition substitution of the carbonyl group and paraposition N led to the chemical shift of C-4 moving to the lower field: 1H -NMR (400 MHz, CD_3OD) δ_H 7.89 (br s, 1H, H-3), 7.67 (br s, 1H, H-5), 4.89 (1H, overlapped, H-7), 2.59 (s, 3H, H-10) and 1.46 (d, $J = 6.6$, H-8); ^{13}C -NMR (100 MHz; CD_3OD) δ_C 168.4 (C-9), 166.9 (C-1), 159.5 (C-6), 142.2 (C-4), 122.6 (C-5), 117.5 (C-3), 71.1 (C-3), 24.4 (C-8), and 23.7 (C-10).

Table 2. The 1H , ^{13}C , HMBC, and HSQC NMR data for compound 7 in CD_3OD .

No.	1H NMR	^{13}C NMR	HMBC	HSQC(δ)
2	—	166.9 (s)	H-3, H-8	—
3	7.89 (1H, br s)	117.5 (d)	H-5	7.89
4	—	142.2 (s)	—	—
5	7.67 (1H, br s)	122.6 (d)	H-3, H-10	7.67
6	—	159.5 (s)	H-10, H-5	—
7	4.89 (1H, overlapped)	71.1 (d)	H-8	4.89
8	1.46 (3H, d, 6.6)	24.4 (q)	H-7	1.36
9	—	168.4 (s)	H-3, H-5	—
10	2.59 (3H, s)	23.7 (q)	H-5	2.59

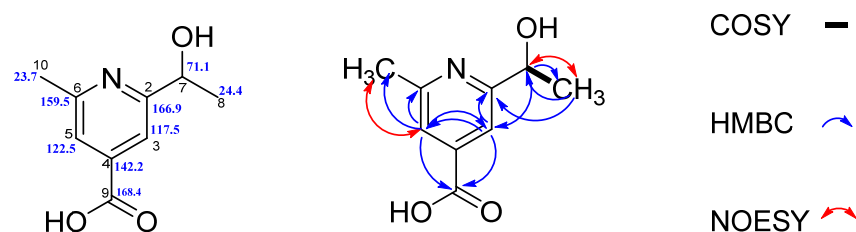


Figure 5. Signal assignment of compound 7 via ^{13}C and 2D NMR.

To confirm the stereochemical assignments of **7**, we carried out the ECD calculation at the PBE0/def2-TZVP level. The experimental ECD spectrum of **7** exhibited a negative Cotton effect at 258 nm ($\Delta\epsilon -10.54$) and a positive Cotton effect at 286 nm ($\Delta\epsilon +7.76$), which displayed strong agreement with the calculated ECD curve of *S*-**7** (Figure 6). Thus, the absolute configuration at the stereogenic center in **7** was (*S*). The structure of compound **7** was determined to be 2-(1-hydroxyethyl)-6-methylisonicotinic acid.

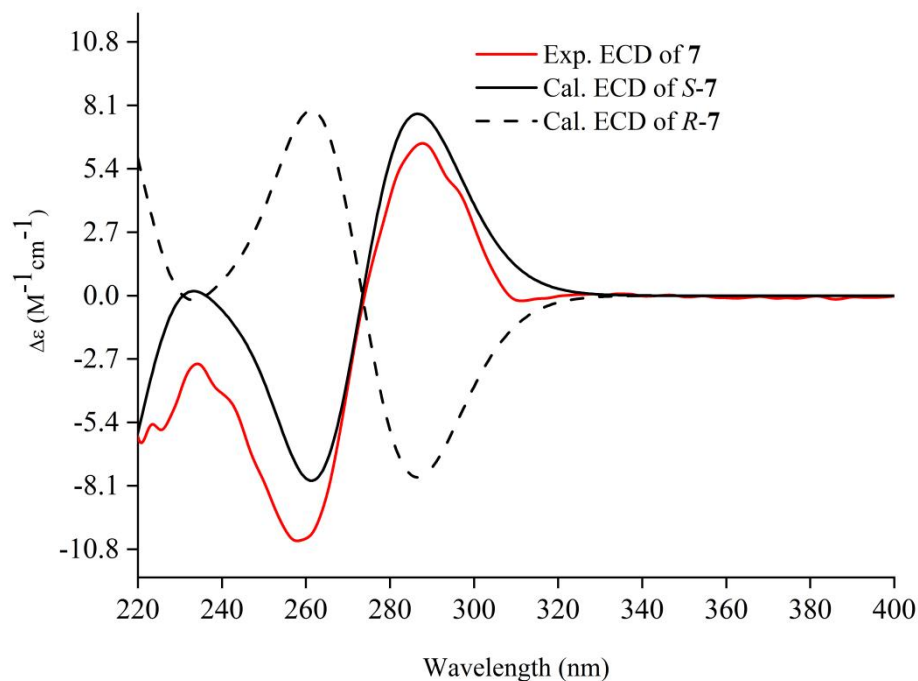


Figure 6. Experimental ECD spectra (200–400 nm) of **7** in methanol and the calculated ECD spectra of the model molecules of **7** at the PBE0/def2-TZVP level.

Compound **9** was isolated as a light yellow powder, and the HR-ESI-MS data showed a molecule peak at m/z 253.0655 $[M + H]^+$ (calculated for $C_{12}H_{13}O_6^+$, 253.0707), which indicated the molecular formula as $C_{12}H_{12}O_6$ and 7 as the index of hydrogen deficiency; 1H -NMR (400 MHz; $DMSO-d_6$) δ_H 1.12–1.14 (d, $J = 6$ Hz, 3H, H-3'), 3.77–3.85 (m, $J = 6.2$ Hz, 1H, H-2'), 3.97–4.00 (t, $J = 5.6$ Hz, 1H, H-3'), 3.75–3.77 (d, 1H, OH), 5.64–5.55 (d, 1H, OH), 6.34 (d, $J = 1.2$ Hz, 1H, H-5), 6.44 (d, $J = 1.2$ Hz, 1H, H-7), 6.61 (s, 1H, H-4), 10.85 (s, 1H, H-6), 11.00 (s, 1H, H-8); and ^{13}C -NMR (400 MHz; $DMSO-d_6$) δ_C 165.5(C-1), 165.3 (C-6), 162.5 (C-8), 157.6 (C-3), 139.2 (C-4a), 104.4 (C-4), 102.9 (C-5), 101.5 (C-7), 97.8 (C-8a), 74.4 (C-1'), 67.4 (C-2'), and 19.7 (C-3') (Figure 7). The 1H -NMR showed that the compound contained one methyl group, two methoxymethyl groups, two alcohol hydroxyl groups, one phenolic hydroxyl group, one phenolic hydroxyl group forming an intramolecular hydrogen bond, and two double-bond protons. The ^{13}C -NMR spectrum ($DMSO-d_6$) of the compound showed 12 carbon signals, including five oxygen-linked aromatic carbons, four oxygen-free aromatic carbons, two oxygen-linked methylene carbons, and one methyl carbon. The unsaturation of the compound was calculated as 6 according to the molecular formula of the compound, and it was inferred that the compound contained two amphioxenic heterocyclic systems. H-7 (δ 6.33) was correlated with C-5 (δ 102.9), C-8a (δ 97.8), C-8 (δ 162.5), and C-6 (δ 165.3), and H-5 was correlated with C-4 (δ 104.4), C-6 (δ 165.3), and C-8a (δ 97.8). Among them, oxygen substitution existed in C-6 (δ 165.3), C-8 (δ 162.5), and C-1 (δ 165.54). According to a comparison of the hydrogen spectra of CD_3OD , C-6 and C-8 are hydroxyl substitutions, and C-1 is the carbonyl group. The abnormal chemical shift of the C-8 hydroxyl group (δ 11.00) indicated that it was greatly shifted to the lower field under the influence of the neighboring carbonyl group. The low-field shift for C-3 (δ 157.6) and the HSQC signal suggested the existence of substitution. On the basis of a

combination with the HMBC and chemical shift characteristics of C-3 and C-1, we inferred that the two carbons were connected by oxygen, resulting in a large chemical shift to the low field (Table 3). On the basis of the above information, we inferred that the compound was a derivative of an isocoumarin skeleton. There was a correlation between C-4, C-3, and C-1, and it was inferred that C-3 had a branched chain substitution: H-1', C-2', C-3', and H-3' were correlated with C-1' and C-2'. A combination of the H spectrum splitting characteristics and hydrogen integral values of H-1, H-2, and H-3 (dd, dq, d peaks; 1H, 1H, 3H, respectively) and the chemical shifts of C-1', C-2', and C-3' (74.4, 67.4, and 19.7, respectively) determined that C-1' and C-2' were hydroxyl substituted and C-3' was a methyl, and the compound signal was assigned. The absolute configurations of compound **9** were established to be 1'R and 2'R by the ECD calculations (Figure 8). Finally, compound **9** was named 6,8-dihydroxy-3-(1'R, 2'R-dihydroxypropyl)-isocoumarin (Figure 1).

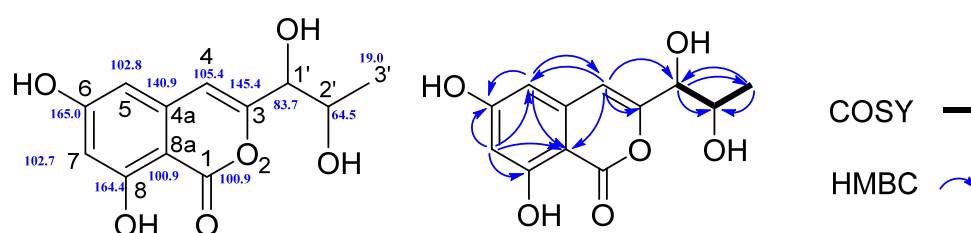


Figure 7. Signal assignment of compound **9** via ^{13}C and HMBC.

Table 3. The ^1H , ^{13}C , HMBC, and HSQC NMR data for compound **9** in DMSO- d_6 .

No.	^1H NMR	^{13}C NMR	HMBC	HSQC
1	—	165.54	—	—
3	—	157.6	H-4	—
4	6.61 (1H, s)	104.4	—	6.61
4a	—	139.2	—	—
5	6.43 (1H, s)	102.9	H-4, H-7	6.43
6	10.88 (OH, s)	165.3	H-7	—
7	6.33 (1H, s)	101.5	—	6.33
8	11.00 (OH, s)	162.5	H-7	—
8a	—	97.8	H-4, H-5, H-7	—
1'	3.97 (1H, dd)	74.7	H-4, H-3'	3.97
2'	3.80 (1H, dq)	67.4	H-1', H-3'	3.80
3'	1.12 (3H, d)	19.7	H-1'	1.12

In addition to the new compounds described above, eight known compounds obtained in this study were identified as compounds **1–3**, **5–6**, **8**, and **10–11** by comparing their spectroscopic data to those reported in the literature. Details of NMR and MS data for compounds **1–11** were given in the Supplementary Materials.

Compound **1** was obtained as a colorless powder, and the HR-ESI-MS data showed a molecule peak at m/z 129.0552 $[\text{M} + \text{H}]^+$ (calculated for $\text{C}_6\text{H}_9\text{O}_3^+$, 129.0546), which indicated a molecular formula of $\text{C}_6\text{H}_8\text{O}_3$ with three degrees of unsaturation. In examining the proton nuclear magnetic resonance (^1H -NMR) data, we found signals for methyl protons δ_{H} 1.41 (3H d, $J = 6.8$ Hz, H- CH_3), one methylene proton δ_{H} 4.28 (2H, d, $J = 1.7$ Hz), and two methines (two oxygenated sp^3 and one sp^2): δ_{H} 5.11–5.16 (1H, m, H-5) and δ_{H} 7.42–7.47 (1H, m, H-4). The ^{13}C -NMR spectra revealed six carbon signals: one ester carbonyl (δ_{C} 174.53), one olefinic methine (δ_{C} 152.93), one nonprotonated sp^2 carbon (δ_{C} 134.75), two oxygenated methines (δ_{C} 80.13), one oxygenated methylene (δ_{C} 56.95), and methyls (δ_{C} 19.02). The structure of **1** was determined as 3-(hydroxymethyl)-5-methylfuran-2(5H)-one [28], as shown in Figure 1.

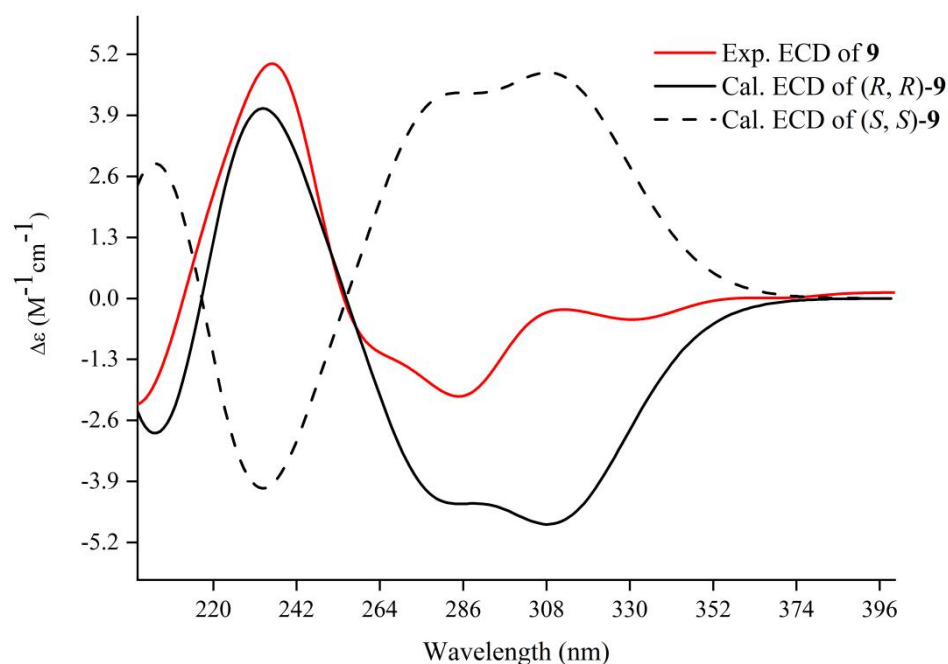


Figure 8. Experimental ECD spectra (200–400 nm) of **9** in methanol and the calculated ECD spectra of the model molecules of **9** at the PBE0/def2-TZVP level.

Compound **2** was a white powder with the molecular formula ($C_7H_8O_4$): HR-ESI-MS m/z 157.0493 $[M + H]^+$ (calculated for $C_7H_9O_4^+$, 157.0495); 1H -NMR (400 MHz, CD_3OD) δ_H 1.33 (d, $J = 6.8$ Hz, 3H, H-CH₃), 5.05–5.09 (m, 1H, H-5), and 7.41–7.45 (m, 1H, H-4); and ^{13}C -NMR (100 MHz, CD_3OD) δ_C 18.93 (C-CH₃), 31.08 (C-2'), 80.00 (C-5), 127.99 (C-3), 155.38 (C-4), 173.10 (C-2), and 175.47 (C-1'). Thus, compound **2** was identified as [2-(5-methyl-2-oxo-2,5-dihydrofuran-3-yl)-acetic acid] by comparing NMR reference data [29]. Previously, compound **2** had only been obtained through chemical synthesis and was isolated as a natural product for the first time [29]. Thus, we named it aspilactonol G.

Compound **3** was a colorless oil with the molecular formula ($C_8H_{10}O_4$): HR-ESI-MS (m/z 171.0654 $[M + H]^+$ (calculated for $C_8H_{10}O_4^+$, 171.0652)). 1H -NMR data (400 MHz, CD_3OD) δ_H 1.33 (d, $J = 6.8$ Hz, 3H, H-5), 5.05–5.09 (m, 2H, H-2), and 7.41–7.45 (m, 1H, H-4); and ^{13}C -NMR (100 MHz, CD_3OD) δ_C 18.92, 30.09, 52.68, 80.05, 127.55, 155.58, 171.64, and 175.25. Thus, compound **3** was identified as [methyl-2-(5-methyl-2-oxo-2,5-dihydrofuran-3-yl)-acetate] by comparing NMR reference data [29]. Compound **3** was also obtained as a natural product for the first time [29]; thus, we named it aspilactonol H.

Compound **5** yielded the following data: HR-ESI-MS m/z 131.0663 $[M + H]^+$ (calculated for $C_6H_{11}O_3^+$, 131.0703); 1H -NMR (400 MHz, CD_3OD) δ_H 2.11 (d, 3H, C-6), 2.30–2.34 (t, 2H, H-4), 3.67–3.70 (t, 2H, H-5), and 5.76 (s, 1H, H-2); and ^{13}C -NMR (400 MHz, CD_3OD) δ_C 18.5, 44.6, 60.9, 120.4, 152.7, and 172.1. Compound **5** is E- Δ^2 -anhydromevalonic acid [30].

Compound **6** yielded the following data: HR-ESI-MS m/z 113.0604 $[M + H]^+$ (calculated for $C_6H_9O_2^+$, 113.0597); 1H -NMR (400 MHz, CD_3OD), δ_H 5.79 (1H, q, $J = 1.5$ Hz, H-3), 4.38 (2H, t, $J = 6.0$ Hz, H-6), 2.41 (2H, br.t, $J = 6.0$ Hz, H-5), and 2.02 (3H, s, H-7); and ^{13}C -NMR (100 MHz, CD_3OD) δ_C 22.6, 28.8, 65.6, 116.2, 158.0, and 164.4. Compound **6** is 4-methyl-5,6-dihydropyren-2-one [31].

Compound **8** was a white amorphous powder. The molecular formula, $C_{10}H_{10}O_4$, was determined by HR-ESI-MS 195.0651 m/z $[M + H]^+$ (calculated for $C_{10}H_{11}O_4^+$, 195.0652) and ^{13}C -NMR data, corresponding to six degrees of unsaturation; 1H -NMR (400 MHz, CD_3OD) δ_H 6.21 (1H, s, H-5), 6.20 (1H, s, H-7), 4.63–4.67 (1H, m, H-3), 2.92 (1H, dd, $J = 16.4$, 3.6 Hz, H-4a), 2.82 (H, dd, $J = 16.4$, 11.2 Hz, H-4b), and 1.45 (3H, d, $J = 6.3$ Hz, H-9); and ^{13}C -NMR (CD_3OD , 100 MHz) δ_C 170.30 (C-1), 164.99 (C-8), 164.23 (C-6), 142.08 (C-4a), 106.53

(C-5), 100.82 (C-8a), 100.0 (C-7), 75.77 (C-3), 34.13 (C-4), and 19.44 (C-9). Compound **8** was identified as (*R*)-6-hydroxymellein [32].

Compound **10**, $C_{11}H_{10}O_4$, was a yellow powder: HR-ESI-MS m/z 207.0651 $[M + H]^+$ (calculated for $C_{11}H_{11}O_4^+$, 207.0652); 1H -NMR (400 MHz, CD_3OD , δ , ppm) δ_H 6.39 (1H, d, $J = 1.5$ Hz, H-7), 6.29 (1H, d, $J = 1.5$ Hz, H-5), 6.24 (1H, s, H-4), 3.78 (3H, s, H-10), and 2.10 (3H, s, H-9); and ^{13}C -NMR (100 MHz, CD_3OD) δ_C 165.1 (C, C-1), 163.6 123 (C, C-8), 158.3 (C, C-6), 155.0 (C, C-3), 142.2 (C, C-4a), 103.5 (CH, C-4), 102.9 (CH, C-5), 100.4 (C, C-8a), 99.2 (CH, C-7), 56.8 (CH₃, C-10), and 19.4 (CH₃, C-9). Compound **10** is 6-hydroxy-8-methoxy-3-methylisocoumarin [33].

Compound **11**, $C_{12}H_{12}O_5$, was a yellow powder: ESI-MS m/z 237.0765 $[M + H]^+$ (calculated for $C_{12}H_{13}O_5^+$, 237.0757); 1H -NMR (400 MHz, CD_3OD , δ , ppm) δ_H 6.40 (2H, d, $J = 2.1$, H-5, 7), 6.37 (1H, d, $J = 2.1$, H-4), 4.69 (1H, m, H-2'), 2.59 (2H, m, H-1'), and 1.26 (3H, d, $J = 6.2$, H-3'); and ^{13}C -NMR (100 MHz, CD_3OD , δ , ppm) δ_C 167.8 (C, C-1), 167.3 (C, C-8), 164.8 (C, C-6), 156.2 (C, C-3), 141.3 (CH, C-4), 107.0 (C, C-7), 103.7 (C, C-10), 102.6 (CH, C-9), 99.8 (CH, C-5), 66.2 (CH, C-2'), 43.8 (CH₂, C-1'), and 23.3 (CH₃, C-3'). The absolute configuration of compound **11** was established to be 2'*R* by the ECD calculations (Figure 9). Thus, compound **11** was identified as de-*O*-methyldiaporthin by comparing NMR reference data [34,35].

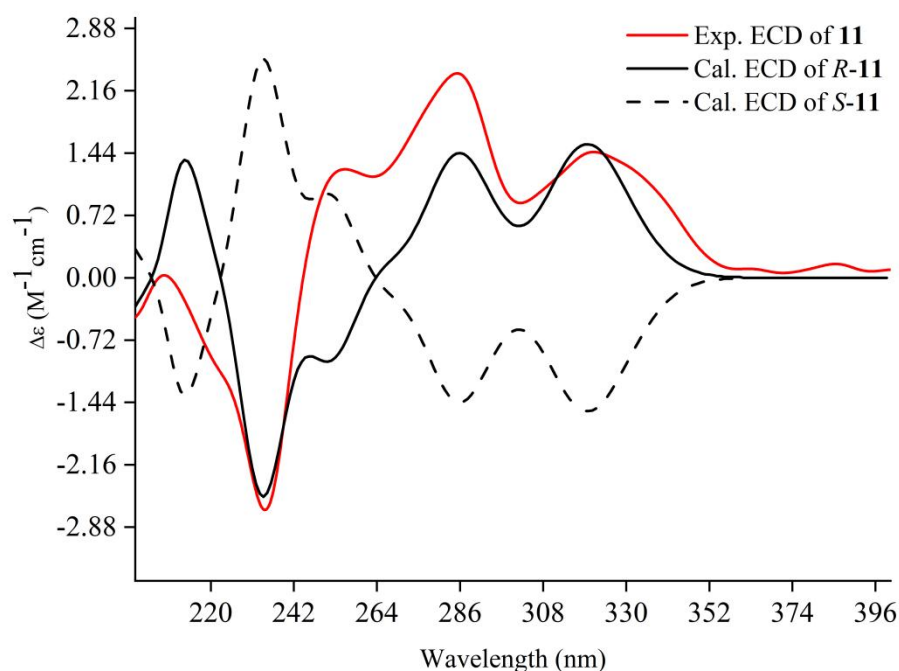
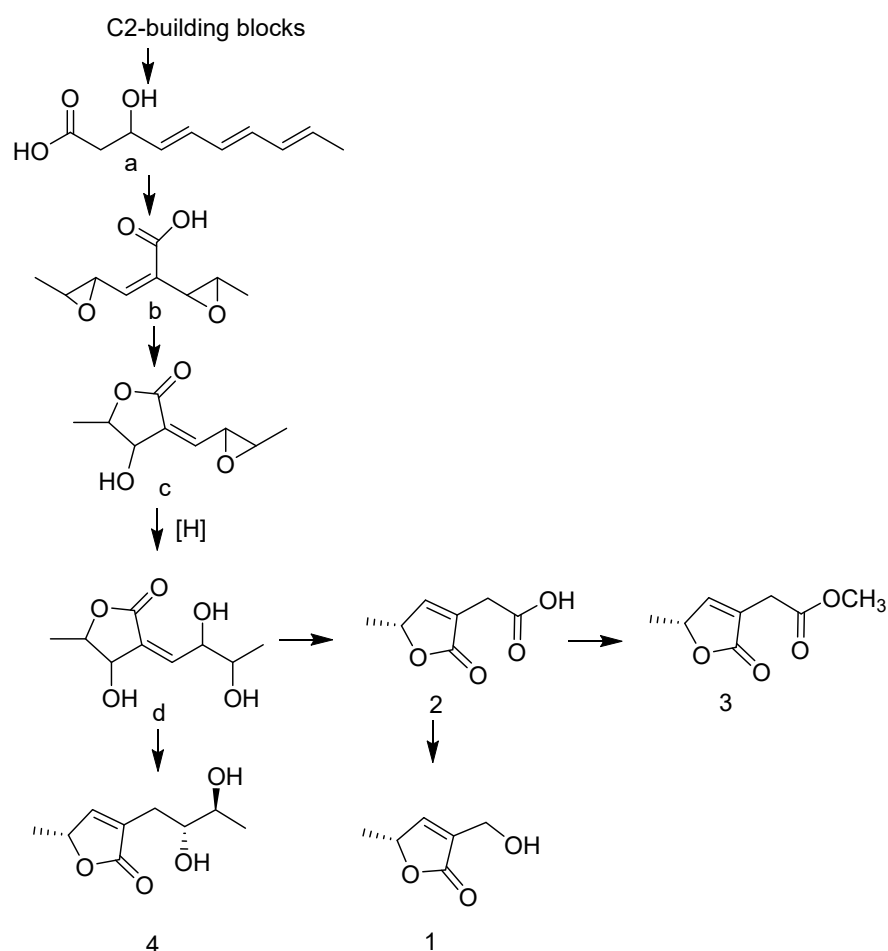


Figure 9. Experimental ECD spectra (200–400 nm) of **11** in methanol and the calculated ECD spectra of the model molecules of **11** at the PBE0/def2-TZVP level.

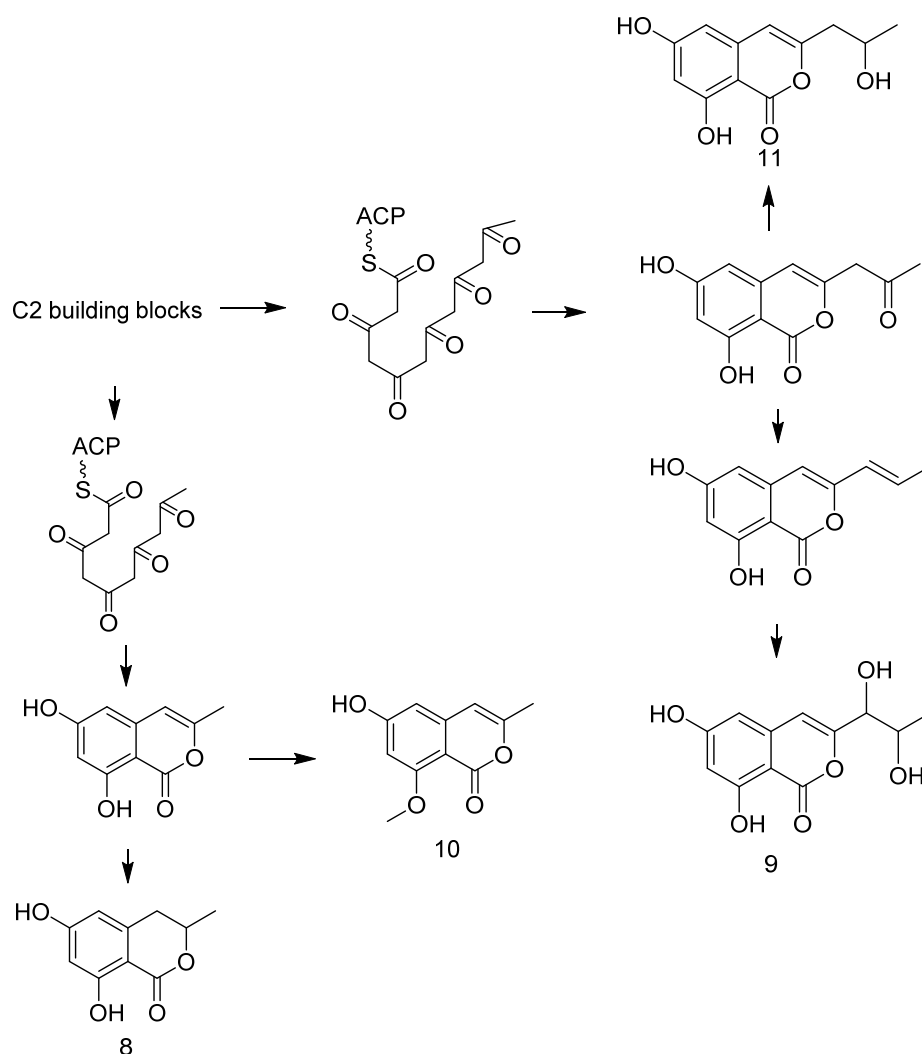
The biosynthesis of the isolated compounds **1–4** and **8–11** was proposed as shown in Schemes 1 and 2, respectively. Furan ring groups are abundant in natural products and play important roles in the pharmacophore of bioactive substances. Furanone and its derivatives have been shown to inhibit the formation of bacterial biofilms; interfere with bacterial population effects; and have analgesic, anti-inflammatory, anticancer, anticonvulsive, antibacterial, antifungal, antioxidation, and other activities. Most of the furanone compounds are synthesized by a single polyketone pathway, although chain fusion of furanone has also been reported in recent years [19,36]. In this study, compounds **4** and **9** possessed *o*-diol side chains. Different carbon skeletons with the same *o*-diol side chains suggested the presence of specific hydroxylating enzymes. A plausible biosynthetic pathway for compounds **1–4** is proposed (Scheme 1). Furanone **1–4** are derivatives of α,β -unsaturated γ -lactone. Their synthesis begins with the condensation of five molecules of acetyl-CoA

to form the intermediate **a**, which is reduced to generate the critical intermediate **b**, and forms the intermediate **c** under the action of cyclase. Then, **c** undergoes ring-opening and oxidation to generate the intermediate **d**, which is dehydrated to produce compound **4**. Compound **2** is synthesized from **d** through an undefined pathway, then methylated to compound **3** and decarboxylated to compound **1** [19,36]. Compounds **8–11** are isocoumarin derivatives (Scheme 2), whose biosynthesis by the polyketone synthesis pathway begins with acetyl-CoA. Isocoumarin derivatives have been detected in both plants and microorganisms. The C-8 of isocoumarins does not have the oxidation found in plants, while the isocoumarins commonly found in microorganisms have oxidation at the C-8 position, which is considered to be the biological source of the two types of isocoumarin [37,38].



Scheme 1. Proposed biosynthetic pathways for furanone compounds (1–4).

The AChE inhibitory activities of the crude extracts were evaluated using Ellman's method, with Rivastigmine and Hup A as the control groups [22,39]. Ethyl acetate, with an inhibition effect value of 82.68%, exhibited better inhibition against AChE than did either petroleum ether extract (47.23%) or buthanol extract (15.82%) (Table S1). In addition, all of the compounds were investigated for their anti-AChE activities. Compounds **1–3** and **5–10** exhibited no inhibitory activity against AChE. Compounds **4** and **11** displayed moderate inhibitory effect on AChE activities with IC_{50} values of 6.26 and 21.18 μ M, respectively (Table 4).



Scheme 2. Proposed biosynthetic pathways for isocoumarin compounds (8–11).

Table 4. Acetylcholinesterase inhibitory activities of the secondary metabolites of *Phaeosphaeria* sp. LF5, expressed as IC_{50} values.

Compound	IC_{50} (μM) ^a	Compounds	IC_{50} (μM) ^a
1	>100	6	>100
2	>100	7	>100
3	>100	8	>100
4	6.26 ± 0.15	9	>100
5	>100	10	>100
Rivastigmine	1.82 ± 0.13	11	21.18 ± 1.53
Hup-A	0.045 ± 0.01		

^a Expressed as the mean \pm SD of three parallel measurements ($p < 0.05$).

Structurally, almost all of the furanone compounds in this study contained an α,β -unsaturated carboxylic acid lactone moiety, which might be the key functional group for their biological activity. De-*O*-methyldiaporthin (11) was first reported in 1988 [34,35]. It can be used as a microbial herbicide due to its very strong phytotoxic activity [40]. AChEIs are drugs that can be used clinically to treat or alleviate symptoms of AD. They are primarily associated with the direction and efficacy of AD drug development based on the cholinergic injury hypothesis. Thus far, two generations of five AChEI drugs (Tacrine, Donepezil, Rivastigmine, Galantamine, and HupA) have been successfully developed

and have become the first choice for clinical treatment or mitigation of AD [10]. Existing clinical AChEI drugs have limitations such as limited efficacy, significant toxicity, and drug resistance. In this study, furanone compound **4** and isocoumarin compound **11** were found to have the potential to inhibit AChE. To the best of our knowledge, furanone compounds were reported here for the first time for their AChE inhibitory activity. Their mechanisms of action and structure–activity relationships in inhibiting AChE require further study by inhibition kinetics analysis and molecular docking methods.

4. Conclusions

To summarize, 11 polyketide derivatives, which included three new compounds, aspilactonol I (**4**), 2-(1-hydroxyethyl)-6-methylisonicotinic acid (**7**), and 6, 8-dihydroxy-3-(1′R, 2′R-dihydroxypropyl)-isocoumarin (**9**), and two new natural-sources-derived aspilactonols (G, H) (**2**, **3**) were isolated from an endophytic fungus *Phaeosphaeria* sp. LF5 of *H. serrata*. Their absolute configurations of three new compounds (**4**, **7**, and **9**) and known compound **11** were determined by ECD calculations. Furanone compound **4** and isocoumarin compound **11** exhibited potent AChE inhibitory activities. This study indicates that *Phaeosphaeria* sp. LF5 from *H. serrata* may contain various AChEI compounds, which is a potential resource pool for bioprospecting and isolating AChEIs. Furthermore, this research also provided a material basis for the development of new and efficient AChEI drugs.

Supplementary Materials: The following supporting information can be downloaded at <https://www.mdpi.com/article/10.3390/jof8030232/s1>. Table S1: Acetylcholinesterase inhibitory activities of the crude extracts, Figure S1: ¹H NMR spectrum of compound **1** in CD₃OD, Figure S2: ¹³C NMR spectrum of compound **1** in CD₃OD, Figure S3: ¹H NMR spectrum of compound **2** in CD₃OD, Figure S4: ¹³C NMR spectrum of compound **2** in CD₃OD, Figure S5: ¹H NMR spectrum of compound **3** in CD₃OD, Figure S6: ¹³C NMR spectrum of compound **3** in CD₃OD, Figure S7: ¹H NMR spectrum of compound **4** in CD₃OD, Figure S8: ¹³C NMR spectrum of compound **4** in CD₃OD, Figure S9: ¹H-¹H COSY spectrum of compound **4** in CD₃OD, Figure S10: DEPT 90 spectrum of compound **4** in CD₃OD, Figure S11: DEPT 135 spectrum of compound **4** in CD₃OD, Figure S12: HSQC spectrum of compound **4** in CD₃OD, Figure S13: HMBC spectrum of compound **4** in CD₃OD, Figure S14: NOESY spectrum of compound **4** in CD₃OD, Figure S15: HRESIMS spectrum of compound **4**, Figure S16: ¹H NMR spectrum of compound **5** in CD₃OD, Figure S17: ¹³C NMR spectrum of compound **5** in CD₃OD, Figure S18: ¹H NMR spectrum of compound **6** in CD₃OD, Figure S19: ¹³C NMR spectrum of compound **6** in CD₃OD, Figure S20: ¹H NMR spectrum of compound **7** in CD₃OD, Figure S21: ¹³C NMR spectrum of compound **7** in CD₃OD, Figure S22: ¹H-¹H COSY spectrum of compound **7** in CD₃OD, Figure S23: HSQC spectrum of compound **7** in CD₃OD, Figure S24: HMBC spectrum of compound **7** in CD₃OD, Figure S25: NOESY spectrum of compound **7** in CD₃OD, Figure S26: HRESIMS spectrum of compound **7**, Figure S27: ¹H NMR spectrum of compound **8** in CD₃OD, Figure S28: ¹³C NMR spectrum of compound **8** in CD₃OD, Figure S29: ¹H NMR spectrum of compound **9** in DMSO-*d*₆, Figure S30: ¹³C NMR spectrum of compound **9** in DMSO-*d*₆, Figure S31: DEPT 90 spectrum of compound **9** in DMSO-*d*₆, Figure S32: DEPT 135 spectrum of compound **9** in DMSO-*d*₆, Figure S33: ¹H-¹H COSY spectrum of compound **9** in DMSO-*d*₆, Figure S34: HSQC spectrum of compound **9** in DMSO-*d*₆, Figure S35: HMBC spectrum of compound **9** in DMSO-*d*₆, Figure S36: NOESY spectrum of compound **9** in DMSO-*d*₆, Figure S37: HRESIMS spectrum of compound **9**, Figure S38: ¹H NMR spectrum of compound **10** in CD₃OD, Figure S39: ¹³C NMR spectrum of compound **10** in CD₃OD, Figure S40: ¹H NMR spectrum of compound **11** in CD₃OD, Figure S41: ¹³C NMR spectrum of compound **11** in CD₃OD.

Author Contributions: Y.X.: conceptualization, methodology, validation, investigation, and writing—original draft; W.L.: investigation, methodology, and validation; S.Z.: data curation and software; Z.Z.: investigation; Y.W.: investigation and methodology; D.Z.: conceptualization, methodology, writing—review and editing, project administration, and funding acquisition; J.L.: resources and methodology; J.C.: resources; C.J.: chemical structure analysis. All authors have read and agreed to the published version of the manuscript.

Funding: This research was supported by the National Natural Science Foundation of China (81760649) and the Natural Science Foundation of Jiangxi Province of China (20181BAB215044).

Institutional Review Board Statement: Not applicable.

Informed Consent Statement: Not applicable.

Data Availability Statement: All data generated or analyzed in this study are available within the manuscript and are available from the corresponding authors upon request.

Conflicts of Interest: The authors declare no conflict of interest.

References

1. Newman, D.J.; Cragg, G.M. Plant endophytes and epiphytes: Burgeoning sources of known and “unknown” cytotoxic and antibiotic agents. *Planta Med.* **2020**, *86*, 13–14. [[CrossRef](#)] [[PubMed](#)]
2. Zou, Z.B.; Zhang, G.; Li, S.M.; He, Z.H.; Yan, Q.X.; Lin, Y.K.; Xie, C.L.; Xia, J.M.; Luo, Z.H.; Luo, L.Z.; et al. Asperochratides A–J, Ten new polyketides from the deep-sea-derived *Aspergillus ochraceus*. *Bioorg. Chem.* **2020**, *105*, 104349. [[CrossRef](#)] [[PubMed](#)]
3. Venugopalan, A.; Srivastava, S. Endophytes as in vitro production platforms of high value plant secondary metabolites. *Biotechnol. Adv.* **2015**, *33*, 873–887. [[CrossRef](#)]
4. Gakuubi, M.M.; Munusamy, M.; Liang, Z.X.; Ng, S.B. Fungal endophytes: A promising frontier for discovery of novel bioactive compounds. *J. Fungi* **2021**, *7*, 786. [[CrossRef](#)]
5. Deshmukh, S.K.; Gupta, M.K.; Prakash, V.; Saxena, S. Endophytic fungi: A source of potential antifungal compounds. *J. Fungi* **2018**, *4*, 77. [[CrossRef](#)]
6. Pal, P.P.; Shaik, A.B.; Begum, A.S. Prospective leads from endophytic fungi for anti-inflammatory drug discovery. *Planta Med.* **2020**, *86*, 941–959. [[CrossRef](#)] [[PubMed](#)]
7. Keshri, P.K.; Rai, N.; Verma, A.; Kamble, S.C.; Barik, S.; Mishra, P.; Singh, S.K.; Salvi, P.; Gautam, V. Biological potential of bioactive metabolites derived from fungal endophytes associated with medicinal plants. *Mycol. Prog.* **2021**, *20*, 577–594. [[CrossRef](#)]
8. Zheng, R.; Li, S.; Zhang, X.; Zhao, C. Biological activities of some new secondary metabolites isolated from endophytic fungi: A review study. *Int. J. Mol. Sci.* **2021**, *22*, 959. [[CrossRef](#)] [[PubMed](#)]
9. Bang, S.; Baek, J.Y.; Kim, G.J.; Kim, J.; Kim, S.J.; Deyrup, S.T.; Choi, H.; Kang, K.S.; Shim, S.H. Azaphilones from an endophytic *Penicillium* sp. prevent neuronal cell death via inhibition of MAPKs and reduction of Bax/Bcl-2 ratio. *J. Nat. Prod.* **2021**, *84*, 2226–2237. [[CrossRef](#)] [[PubMed](#)]
10. Cao, D.; Sun, P.; Bhowmick, S.; Wei, Y.H.; Guo, B.; Wei, Y.H.; Mur, L.A.J.; Sun, Z.L. Secondary metabolites of endophytic fungi isolated from *Huperzia serrata*. *Fitoterapia* **2021**, *155*, 104970. [[CrossRef](#)] [[PubMed](#)]
11. Wang, Y.; Lai, Z.; Li, X.X.; Yan, R.M.; Zhang, Z.B.; Yang, H.L.; Zhu, D. Isolation, diversity and acetylcholinesterase inhibitory activity of the culturable endophytic fungi harboured in *Huperzia serrata* from Jinggang Mountain, China. *World J. Microbiol. Biotechnol.* **2016**, *32*, 20. [[CrossRef](#)] [[PubMed](#)]
12. Wang, Y.; Zeng, Q.G.; Zhang, Z.B.; Yan, R.M.; Zhu, D. Isolation and characterization of endophytic huperzine a-producing fungi from *Huperzia serrata*. *J. Ind. Microbiol. Biotechnol.* **2010**, *38*, 1267–1278. [[CrossRef](#)] [[PubMed](#)]
13. Singh, S.B.; Ondeyka, J.; Harris, G.; Herath, K.; Zink, D.; Vicente, F.; Bills, G.; Collado, J.; Platas, G.; González del Val, A.; et al. Isolation, structure, and biological activity of phaeofungin, a cyclic lipodepsipeptide from a *Phaeosphaeria* sp. using the genome-wide *Candida albicans* fitness test. *J. Nat. Prod.* **2013**, *76*, 334–345. [[CrossRef](#)] [[PubMed](#)]
14. Karakoyun, Ç.; Küçüksoğlak, M.; Bilgi, E.; Doğan, G.; Çömlekçi, Y.E.; Bedir, E. Five new cardenolides transformed from oleandrin and nerigoside by *Alternaria eureka* 1e1b1 and *Phaeosphaeria* sp. 1e4cs-1 and their cytotoxic activities. *Phytochem. Lett.* **2021**, *41*, 152–157. [[CrossRef](#)]
15. Zhan, Z.J.; Jin, J.P.; Ying, Y.M.; Shan, W.G. Furanone derivatives from *Aspergillus* sp. xw-12, an endophytic fungus in *Huperzia serrata*. *Helv. Chim. Acta* **2011**, *94*, 1454–1458. [[CrossRef](#)]
16. Husain, A.; Khan, S.A.; Iram, F.; Iqbal, M.A.; Asif, M. Insights into the chemistry and therapeutic potential of furanones: A versatile pharmacophore. *Eur. J. Med. Chem.* **2019**, *191*, 66–92. [[CrossRef](#)] [[PubMed](#)]
17. Yurchenko, A.N.; Trinh, P.T.H.; Ivanets, E.V.G.; Smetanina, O.F.; Afiyatullo, S.S. Biologically active metabolites from the marine sediment-derived fungus *Aspergillus flocculosus*. *Mar. Drugs* **2019**, *17*, 579. [[CrossRef](#)] [[PubMed](#)]
18. Liu, Y.; Li, X.M.; Meng, L.H.; Wang, B.G. Polyketides from the marine mangrove-derived fungus *Aspergillus ochraceus* MA-15 and their activity against aquatic pathogenic bacteria. *Phytochem. Lett.* **2015**, *12*, 232–236. [[CrossRef](#)]
19. Hu, H.C.; Li, C.Y.; Tsai, Y.H.; Yang, D.Y.; Chang, F.R. Secondary metabolites and bioactivities of *Aspergillus ochraceopetaliformis* isolated from *Anthurium brownii*. *ACS Omega* **2020**, *5*, 20991–20999. [[CrossRef](#)] [[PubMed](#)]
20. Tianpanich, K.; Prachya, S.; Wiyakrutta, S.; Mahidol, C.; Ruchirawat, S.; Kittakoop, P. Radical scavenging and antioxidant activities of isocoumarins and a phthalide from the endophytic fungus *Colletotrichum* sp. *J. Nat. Prod.* **2011**, *74*, 79–81. [[CrossRef](#)] [[PubMed](#)]
21. Gao, W.; Wang, X.; Chen, F.; Li, C.; Cao, F.; Luo, D. Setosphalides A–D, New Isocoumarin Derivatives from the Entomogenous Fungus *Setosphaeria rostrata* LGWB-10. *Natur. Prod. Biopros.* **2021**, *11*, 137–142. [[CrossRef](#)]
22. Ellman, G.L.; Courtney, K.D.; Andres, V.; Featherstone, R.M. A new and rapid colorimetric determination of acetylcholinesterase activity. *Biochem. Pharmacol.* **1961**, *7*, 88–95. [[CrossRef](#)]

23. Ortiz, J.E.; Berkov, S.; Pigni, N.B.; Theoduloz, C.; Roitman, G.; Tapia, A.; Bastida, J.; Feresin, G. Wild Argentinian Amaryllidaceae, a new renewable source of the acetylcholinesterase inhibitor galanthamine and other alkaloids. *Molecules* **2012**, *17*, 13473–13482. [CrossRef] [PubMed]
24. *Sybyl Software*; Version X 2.0; Tripos Associates Inc.: St. Louis, MO, USA, 2013.
25. Neese, F. The ORCA program system. *WIREs Comput. Mol. Sci.* **2012**, *2*, 73–78. [CrossRef]
26. Neese, F. Software update: The ORCA program system, version 4.0. *WIREs Comput. Mol. Sci.* **2017**, *8*, e1327. [CrossRef]
27. Stephens, P.J.; Harada, N. ECD cotton effect approximated by the Gaussian curve and other methods. *Chirality* **2010**, *22*, 229–233. [CrossRef] [PubMed]
28. National Center for Biotechnology Information. PubChem Compound Summary for CID 234614, 3-(Hydroxymethyl)-5-methylfuran-2(5h)-one. 2022. Available online: https://pubchem.ncbi.nlm.nih.gov/compound/3-Hydroxymethyl-5-methylfuran-2_5h-one (accessed on 24 January 2022).
29. Patel, R.M.; Puranik, V.G.; Argade, N.P. Regio- and stereoselective selenium dioxide allylic oxidation of (E)-dialkyl alkylidenesuccinates to (Z)-allylic alcohols: Synthesis of natural and unnatural butenolides. *Org. Biomol. Chem.* **2011**, *9*, 6312–6322. [CrossRef] [PubMed]
30. Widmer, J.; Keller-Schierlein, W. Stoffwechselprodukte von Mikroorganismen. 139. Mitteilung. Synthesen in der Sideramin-Reihe: Rhodotorulasäure und Dimerumsäure. *Helv. Chim. Acta* **1974**, *57*, 1904–1912. [CrossRef]
31. Li, L.J.; Tao, M.H.; Chen, Y.C.; Zheng, C.X.; Huo, G.H.; Zhang, W.M. Secondary metabolites from the solid culture of marine fungal strain *Penicillium sclerotiorum* FS50. *Mycosystema* **2015**, *34*, 117–123. Available online: http://en.cnki.com.cn/Article_en/CJFDTOTAL-JWXT201501016.htm (accessed on 12 January 2022).
32. de Sá, J.D.M.; Pereira, J.A.; Dethoup, T.; Cidade, H.; Sousa, M.E.; Rodrigues, I.C.; Costa, P.M.; Mistry, S.; Silva, A.M.S.; Kijjoo, A. Anthraquinones, diphenyl ethers, and their derivatives from the culture of the marine sponge-associated fungus *Neosartorya spinosa* KUFA 1047. *Mar. Drugs* **2021**, *19*, 457. [CrossRef] [PubMed]
33. Feng, L.X.; Zhang, B.Y.; Zhu, H.J.; Pan, L.; Cao, F. Bioactive metabolites from *Talaromyces purpureogenus*, an endophytic fungus from *Panax notoginseng*. *Chem. Nat. Comp.* **2020**, *56*, 974–976. [CrossRef]
34. Hallock, Y.F.; Clardy, J.; Kenfield, D.S.; Strobel, G. De-O-methyladioporthin, a phytotoxin from *Drechslera siccans*. *Phytochemistry* **1988**, *27*, 3123–3125. [CrossRef]
35. Zhang, X.Q.; Qu, H.R.; Bao, S.S.; Deng, Z.S.; Guo, Z.Y. Secondary metabolites from the endophytic fungus *Xylariales* sp. and their antimicrobial activity. *Chem. Nat. Comp.* **2020**, *56*, 530–532. [CrossRef]
36. Chen, X.W.; Li, C.W.; Cui, C.B.; Hua, W.; Zhu, T.J.; Gu, Q.Q. Nine new and five known polyketides derived from a deep sea-sourced *Aspergillus* sp. 16-02-1. *Mar. Drugs* **2014**, *12*, 3116–3137. [CrossRef]
37. Hussain, H.; Green, I.R. A patent review of two fruitful decades (1997–2016) of isocoumarin research. *Expert Opin. Ther. Pat.* **2017**, *27*, 1267–1275. [CrossRef]
38. Xiang, P.; Ludwig-Radtke, L.; Yin, W.B.; Li, S.M. Isocoumarin formation by heterologous gene expression and modification by host enzymes. *Org. Biomol. Chem.* **2020**, *18*, 4946–4948. [CrossRef]
39. Sonmez, F.; Zengin Kurt, B.; Gazioglu, I.; Basile, L.; Dag, A.; Cappello, V.; Ginex, T.; Kucukislamoglu, M.; Guccione, S. Design, synthesis and docking study of novel coumarin ligands as potential selective acetylcholinesterase inhibitors. *J. Enzyme Inhib. Med. Chem.* **2017**, *32*, 285–297. [CrossRef]
40. Yuan, C.; Guo, Y.H.; Li, G.; Wu, C.S.; Li, M. Metabolites of endophytic fungus *Elaphocordyceps* sp. *Microbiol. China* **2014**, *41*, 857–861.